Letter of Intent
for
Hyperon-Proton Scattering Experiments
at the 50-GeV PS

M. Ieiri
KEK, Japan
K. Imai
Kyoto University, Japan
B. Bassalleck
University of New Mexico, USA
P. Tlusty
Nuclear Physics Institute, Czech republic

January 10, 2003

Contents

1 Introduction

Studies of the interactions among baryons are essential in understanding "QCD-inspired" pictures of strong interactions in nuclear physics. The nucleon-nucleon (NN) interactions have been extensively studied both theoretically and experimentally, but not much is known about the hyperon-nucleon (YN) interactions.

Nucleon-nucleon (NN) scattering was extensively studied in the 50's and 60's. The existence of a "hard-core" has been verified definitely by a phase-shift analysis, and the NN scattering data have been well described by one-boson exchange (OBE) models. The OBE models have been extended to include the YN sector to understand the NN interaction as the strong interaction between the baryon octet. The Nijmegen group took into account the flavor SU(3) symmetry [1] and the Bonn-Julich group developed a model based on SU(6) symmetry [2]. On the other hand, the short-range repulsive force of the strong interaction has been tried to be explained based on a more basic hierarchy, i.e., quarks and gluons. The quark-cluster model approach has been developed by groups from Tokyo, Tubingen and Kyoto-Niigata [3, 4, 5]. They successfully produced the "core" and predicted several interesting features such as strong isospin dependence of the interactions and the anti-symmetric spin-orbit force.

While we have thus seen a rapid theoretical progress in several pictures [1, 2, 3, 4, 5] of the baryon-baryon (BB) interaction, experimental investigations [6] for the YN interactions were very sparse and have fallen behind theory except for a present trial at KEK in the strangeness S=-1 YN system [7, 8]. In order to scrutinize these theoretical models and to further understand the BB interaction, one has to extend his playground to the YN sector, since an additional degree of strangeness and the Pauli principle on the quark level are expected to give an important aspect. In the BB interaction, it seems to be difficult to incorporate both the boson exchange and the quark-gluon treatments due to the lack of the experimental effort. So, by getting reliable and accurate YN scattering data, one should like to settle a model based on QCD or SU(3) framework, especially for explaining the short range part and the l·s strength. And if lucky, one can detect a "quark effects" as the limits of the conventional picture. YN scattering data will play a key role to get the right picture of the B-B interaction. Intense pion and kaon beam in 1$\sim$ 2 GeV/c region at the 50 GeV PS plays an important role for the progress of this subject.

2 Yp scattering

Hyperon-proton (Yp) scatterings are summarized in the table 1. For each hyperon, its production reactions, Yp scatterings and successive hyperon decays are displayed. As for Λp, Σ^+p, Σ^-p and Ξ^-p elastic scattering, charged particles take part in all the processes, then these channels would be tractable. However, reaction channels such as Σ^-p$\rightarrow$ Σ^0n, Ξ^-p$\rightarrow$ Ξ^0n, might not be tangible, since more than one γ's and/or neutrons appear in the processes. Channels, which are marked by star, can be reconstructed kinematically, if we detect all the charged particles in the production, scattering and decays.

	cτ [cm]	production reaction	(σ[μb] @P[GeV/c])	outgoing particle	**Y-p scattering**	scattered particle		decay mode	α	decay particles	
Λ	7.89	π^-p → K$^0\Lambda$	(700 @1.0)	$\pi^+\pi^-$	**Λp → Λp**	p	Λ	→ pπ^-	0.642	p, π^-	★
		K^-p → $\pi^0\Lambda$	(3500@0.9)	2γ				→ nπ^0	0.65	n, 2γ	
					→ Σ^{0}p	p	Σ^0	→ Λ γ		p, π^-, n, 2γ , γ	★
Σ$^+$	2.396	π^+p → K$^+\Sigma^+$	(500 @1.6)	K^+	**Σ$^+$p → Σ$^+$p**	p	Σ$^+$	→ pπ^0	–0.980	p, 2	★
		K^-p → $\pi^-\Sigma^+$	(1500@1.2)	π^-				→ nπ^+	0.068	n, π^+	★
Σ$^-$	4.434	π^-p → K$^+\Sigma^-$	(250 @1.5)	K^+	**Σ$^-$p → Σ$^-$p**	p	Σ$^-$	→ nπ^-	–0.068	n, π^-	★
		K^-p → $\pi^+\Sigma^-$	(1500@1.0)	π^+	**→ Λn**	n	Λ	→ pπ^-	0.642	p, π^-	★
								→ nπ^0	0.65	n, 2γ	
					→ Σ^{0}n	n	Σ^0	→ Λ γ		p, π^-, γ n, 2γ , γ	
Σ^0	2.22×10^{-9}										
Ξ^0	8.71	K^-p → K$^0\Xi^0$	(90 @1.6)	$\pi^+\pi^-$	**Ξ^{0}p → Ξ^{0}p**	p	Ξ^0	→ Λπ^0	–0.411	p, π^-, 2γ n, 2γ , 2γ	
Ξ$^-$	4.91	K^-p → K$^+\Xi^-$	(160 @1.6)	K^+	**Ξ$^-$p → Ξ$^-$p**	p	Ξ$^-$	→ Λπ^-	–0.456	p, π^-, π^- n, 2γ , π^-	★
					→ ΛΛ	Λ	Λ	→ pπ^-	0.642	p, π^-, p, π^-	★
								→ nπ^0	0.65	p, π^-, n, 2γ	
					→ Ξ^{0}n	n	Ξ^0	→ Λπ^0	–0.411	p, π^-, 2γ n, 2γ 2γ	

Table 1: List of hyperon-proton scattering.

In this letter of intent, we should like to propose two important experimental subjects as a first step; Ξ^-p→ ΛΛ reaction to study the interaction in the S=−2 sector directly, and asymmetry measurement in Λp and Σ^+p elastic scatterings to investigate the anti-symmetric spin-orbit strength.

3 Ξ^-p→ ΛΛ reaction

3.1 Physics interests

We propose to measure the energy dependence of the Ξ^-p→ ΛΛ reaction at the Ξ^- momenta below 1 GeV/c to study the ΛΛ interaction by the ΛΛ invariant mass and the differential cross section.

In the S=−2 sector, the H dibaryon was first predicted by Jaffe as a six-quark state bound by the color-magnetic interaction [9]. Although several experimental efforts have been made [10], the existence of the H is still an open question. The H-dibaryon is suggested

to be very loosely bound, or unbound, relative to $2m_\Lambda$ by the observation of double Λ-hypernuclear events [11], or could be resonance by recent theoretical estimates [12]. In the theoretical frameworks, H particle can exist only in a quark picture, not in any OBE models. Thus, the characteristic features of a "core" region are different largely between the QCM and the OBE especially in S=−2. Since the direct production of the H-dibaryon seems to be very hard, Ξ^-p scattering experiment below 1 GeV/c will play an important role in the understanding of the short range part of the baryon-baryon interaction at S=−2.

The S=−2 baryon-baryon interaction can be studied also through the double Λ hypernuclei and Ξ-hypernuclei. The double Λ hypernuclei has been found in the KEK E176 hybrid-emulsion experiment [11]. The new emulsion-counter hybrid experiment at KEK-E373 [13] has been obtained clear events of double Λ hypernuclei. The experiment to detect several hundreds double Λ hypernuclei by observing characteristic π^- mesonic decays [14] was also performed at BNL as E906. These double Λ hypernuclei study and the Ξ^-p scattering experiment proposed here are complementary each other in understanding of the baryon-baryon interaction at S=−2. A measurement of the Ξ^-p→ $\Lambda\Lambda$ cross section is crucial in assessing the stability of Ξ quasi-particle states in the nucleus.

3.2 Experiment

The production cross section of the Ξ^- is ten times smaller than the Σ and Λ case, so intense K^- beam for its production is needed to obtain a sufficient number of scattering events for Ξ^-. Here, we expect the beam intensity of 10^7 K^-/sec with a good K/π ratio better than 1 at 1.7 GeV/c.

The S=−1 YN scattering experiment at KEK utilized a plastic scintillating fiber block (SCIFI detector) [7] or a liquid scintillating with a track image camera (SCITIC detector) [8] as a live target for the hyperon production and scattering . However, the maximum acceptable rate of these image detectors at present is 10^5 Hz, which is limited by decay time of the phosphor of the first image intensifier tube (IIT). Therefore, at the 50 GeV PS, this IIT technique cannot be used in a Ξ^-pscattering experiment so far.

A schematic drawing around the target region is shown in Fig. 1. The shape of K^- beam is required to be thin (about 1 mm) in the vertical direction. A liquid hydrogen of 20 cm long, 5 cm wide and 1 cm high is used as a production target of the Ξ^- via the $K^-p\rightarrow K^+\Xi^-$ reaction. The produced Ξ^-'s are identified by tagging K^+'s in the forward K^+ spectrometer. The center of the K^+ spectrometer is located at 25 degrees beneath the K^- beam axis to produce the Ξ^- upwards in the production angle around 27 degrees in the laboratory frame as shown in Fig. 2. The Ξ^- beam with wide kinetic energy range below 400 MeV is produced through the 5 mm thick tungsten energy-degrader. Another liquid hydrogen of 2 cm high is put on the tungsten as a scattering target of Ξ^-p interactions. Fig. 3(a) shows a momentum distribution of Ξ^- just before its decay versus its vertical decay position. The kinetic energy of the Ξ^- beam after tungsten degrader is shown in Fig. 3(b), which covers below 400 MeV.

A cylindrical drift chamber system (CDS), which is similar to the system of the BNL-AGS E906 [14], will be applied covering above a scattering target region to detect charged

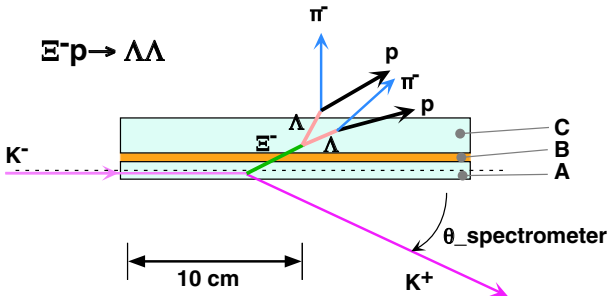

Figure 1: Schematic drawing of a traget region. A liquid hydrogen of 20 cm long, 5cm wide and 1 cm high is used as a production target of the Ξ^-. A: 10 mm thick liquid H_2, B: 5 mm thick tungsten degrader, C: 20 mm thick liquid H_2. The Ξ^- beam with wide kinetic energy range below 400 MeV is produced through the 5 mm thick tungsten energy-degrader. Another liquid hydrogen of 2 cm high is put on the tungsten as a scattering target of Ξ^-p interactions.

particles related to the Ξ^-p interactions as shown in Fig. 4. Some of Ξ^-'s interact with another proton in the liquid hydrogen scattering target. Both (A) elastic scatterings Ξ^-p→ Ξ^-p (Isospin; T=0, 1) and (B) reaction Ξ^-p→ ΛΛ (T=0) are available.

$$\begin{array}{lllll} (A) & \Xi^- p \to \Xi^- \underline{p} & ; & \Xi^- \to \Lambda \underline{\pi}^- \ (100\%) & \Lambda \to \underline{p}\underline{\pi}^- \ (64\%) \\ (B) & \Xi^- p \to \Lambda\Lambda & ; & \Lambda \to \underline{p}\underline{\pi}^- \ (64\%) & \Lambda \to \underline{p}\underline{\pi}^- \ (64\%) \end{array}$$

Charged-particles related to these Ξ^-p interactions (underlined particles in (A) and (B)) should be detected by the CDS to reconstruct its reaction kinematics. For both channels, final charged particles to be detected are two protons and two negative-pions.

Events, which have 4 charged-particles' trajectories by the CDS, are analyzed as Ξ^-p interaction candidates. Protons and π^-'s will be determined well by a mass analysis by tracking of their particle trajectories and TOF information from hodoscopes under a solenoidal magnetic field of 5 kG at the CDS. All 4 particles in this event will be identified as p or π^- by this mass analysis and their momentum can be obtained from trajectories in the CDS.

Next, Λ('s) will be identified by the "invariant mass" analysis for two "p" and "π^-" combinations. If single Λ is assigned from two protons and two π^-'s and then $\Xi^-$are identified with this Λ and a remaining π^-, this event is a candidate of the Ξ^-p→ Ξ^-p elastic scattering. If two Λ's can be identified and a Ξ^- cannot be assigned from any combination with one of these Λ and π^-, the event is a candidate of the reaction Ξ^-p→ ΛΛ(Fig. 5). The kinematic fitting will be performed for these candidates of the Ξ^-p interaction to confirm the kinematics of (A) or (B).

3.3 Identification efficiency of events

The identification rate in the analysis described here was evaluated in the work at the AGS proposal P928 [16]. We refer to values at that work, since we assume the similar CDS de-

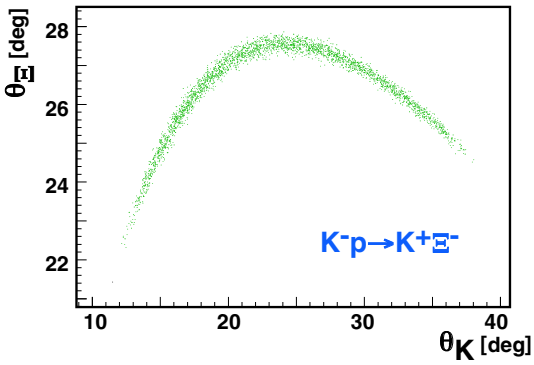

Figure 2: Ξ^- production angle vs K^+ outgoing angle. The center of the K^+ spectrometer is located at 25 degrees beneath the K^- beam axis to produce the Ξ^- upwards in the production angle around 27 degrees in the laboratory frame.

tector system for two protons and two negative-pions after the Ξ^-p scattering.

· **Misidentification of "Λ" and "Ξ^-"**

Events, with 4 charged-particles' trajectories by the CDS, will be analyzed. After the Ξ^-p interaction in the scattering target, 10% of the elastic scattering (A) and 8.8% of the reaction (B) will satisfy this condition.

As described in the previous section, the final state of the Ξ^-p interaction (Ξ^-p or $\Lambda\Lambda$) will be determined by the invariant mass analysis from 4 particles detected by the CDS. In the identification procedure of "Λ", some will be misidentified.

The average momentum resolution of the CDS is assumed to be 1% for π^- and 3% for p, respectively, in each kinematical region of the Ξ^-p interaction. For a miscombination, e.g. the combination of a recoil-proton and a decay- π^- from Ξ^-p after the elastic scattering (A) (Fig. 6), 32.9% of this combination will be assigned as "Λ" in the mass analysis (m_Λ-15 $< m < m_\Lambda$+15 [MeV/c^2]) under this momentum resolution. For the reaction (B), 31.1% of the combination by a Λ and a $\pi^-$are also misidentified as "Ξ^-" ($m_{\Xi^-}-15 < m < m_{\Xi^-}+15$ [MeV/c^2]).

After the invariant mass analysis of possible combinations of particles, the identification efficiencies of the final states are obtained as Table 2. Events which can be interpreted as both Ξ^-p and $\Lambda\Lambda$ will be discarded.

· **Backgrounds from free Ξ^- decay**

Almost all Ξ^-'s decay in flight in the target region, that is, 30% of produced Ξ^-'s decay to $\Lambda\pi^-$ in the target and 20% of these Λ's decay to pπ^- in the scattering liquid hydrogen target. If one of these decay products scatters elastically with proton in the target again, final particles of this event are two p's and two π^-'s same as Ξ^-p interactions as shown in Fig. 7. The rate of these elastic scatterings will be comparable to the Ξ^-p interaction in the liquid hydrogen target. Some of these events will also satisfy the analysis condition; 4

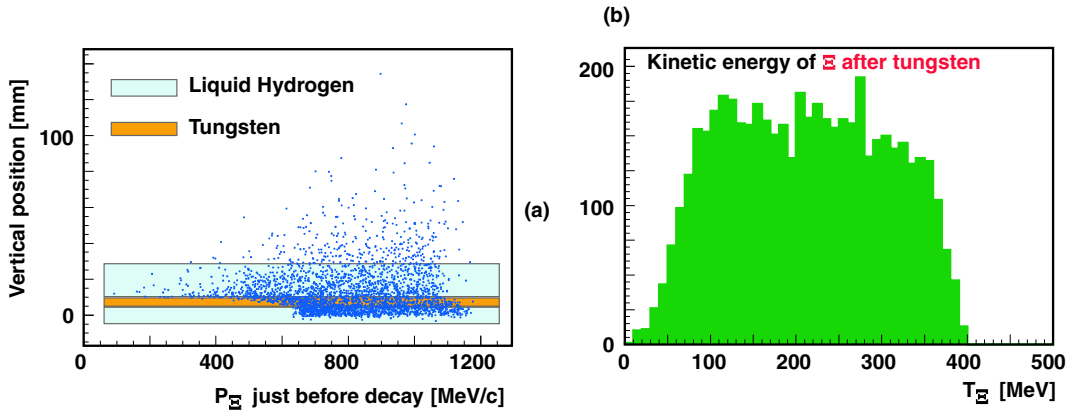

Figure 3: (a) Momentum distribution of Ξ^- just before its decay versus its vertical decay position. (b) The kinetic energy of the Ξ^- beam after tungsten degrader, which covers below 400 MeV.

Final states	Real event: [A] $\Xi^-p \rightarrow \Xi^-p$
Identified as Ξ^-p	65 %
Both Ξ^-p and are possible	35 %
Final states	Real event: [B] $\Xi^-p \rightarrow \Lambda\Lambda$
Identified as $\Lambda\Lambda$	50 %
Both Ξ^-p and are possible	50 %

Table 2: Identification efficiencies of the final states for each reaction.

charged-particles' trajectories by the CDS. Therefore, these could be a source of backgrounds of this experiment.

(i) π^--p elastic scattering [Fig. 7 (a), (b)]

For a combination of π^- and p, we can try to calculate initial "π^-" mass from momenta of these $\pi^-$and p if we assume π^-p elastic scattering. However, for any combinations of π^- and p resulting from Ξ^-p interactions (A) and (B), one cannot obtain this "π^-" mass (for these cases, the calculated $\langle$"π^-" mass$\rangle^2$ gives negative value for any combinations in this case). Then, events which will give the real "π^- mass" in this calculation come from π^-p elastic scattering in Fig. 7 (a) and (b). This check will eliminate events which include π^-p elastic scattering.

(ii) pp and Λp scattering [Fig. 7 (c), (d)]

As for (c) and (d) (also for (b)) in Fig. 7, decay π^- from Ξ^- goes out through the target without scattering. For these cases, mass of decay Λ from Ξ^- will be obtained by using the initial Ξ^- momentum from the (K^-,K^+) reaction and the momentum of one of π^- in the final particles detected by the CDS. For real Ξ^-p interactions, 25% of events satisfy this "Λ" mass (m_Λ-15 < m < m_Λ+15 [MeV/c^2]) which is calculated from initial Ξ^- and one of two

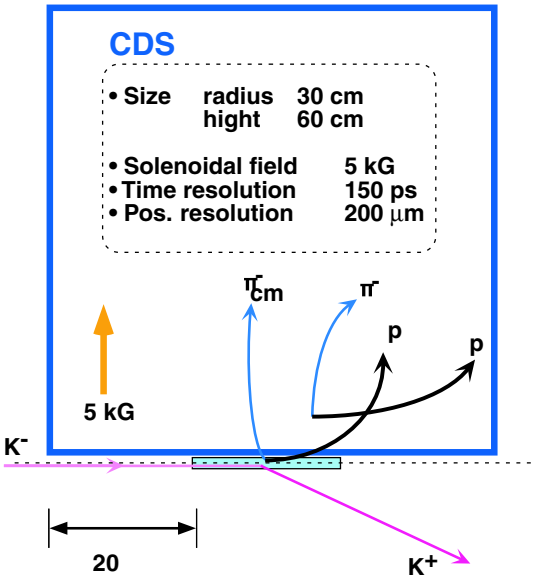

Figure 4: Schematic drawing of a cylindrical drift chamber system (CDS).

π^- as shown in Fig. 7. After this procedure, 85% of real Ξ^-p interactions will survive.

Finally, 4.9% (= 10% × 65% × 75%) of the elastic scattering (A) and 3.3% (= 8.8% × 50% × 75%) of the reaction (B) will survive among all Ξ^-p interactions in the liquid hydrogen target.

3.4 Expected yield

The rate of the Ξ^-p hyperon production is expressed as:

$$Y_{\Xi^-} = n_{K^-} \cdot n_p \cdot \frac{d\sigma}{d\Omega}(K^- p \to K^+ \Xi^-) \cdot d\Omega_{Spectrometer} \cdot \eta_{K^+}$$

where,

n_{K^-}	number of incident K^- : 10^7 /sec
n_p	number of proton target
	8.5×10^{23}protons/cm^2 in the 20 cm liquid hydrogen
$\frac{d\sigma}{d\Omega}(K^- p \to K^+ \Xi^-)$	differential cross section for production [17]
$d\Omega_{Spectrometer}$	solid angle of the spectrometer
	40 cm wide and 20 cm high window at 1 m distance
η_{K^+}	survival rate of K^+ at TOF wall: 0.51 at 5 m

The production rate of Ξ^-, i.e. a rate of the (K^-,K^+) reaction, is 11 per second (9.7×10^7 Ξ^- in total of 100 days machine time). Next, the expected yields of the elastic scattering of Ξ^-p and the reaction Ξ^-p→ ΛΛ in the 2 cm high liq. hydrogen target are expressed as:

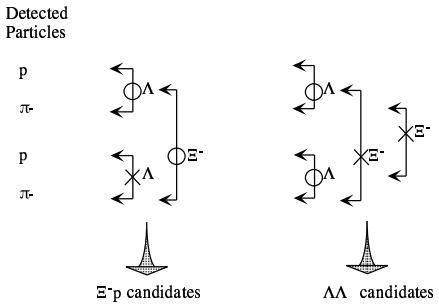

Figure 5: Procedure of assignment of the final state by the invariant mass analysis.

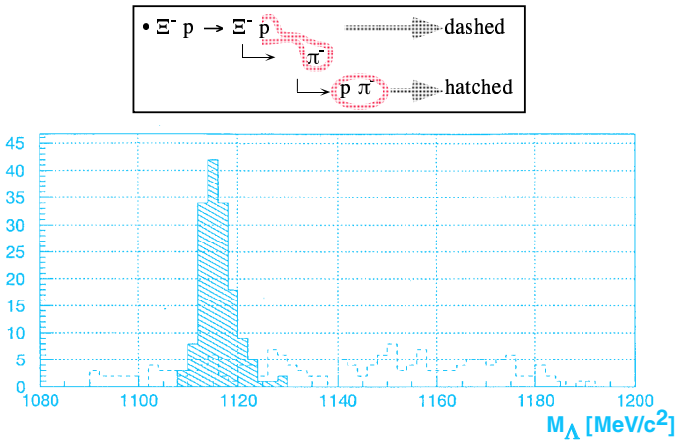

Figure 6: Invariant mass spectrum for the several combinations. "Λ" ; a correct combination, i.e. p and π^- from Λ decay (hatched), and a wrong combination of recoil-p and π^- from Ξ^- decay (dashed).

$$Y_{\Xi^- p \to \Xi^- p, \Lambda\Lambda} = Y_{\Xi^-} \cdot n_{p-eff} \cdot \frac{d\sigma}{d\Omega}(\Xi^- p \to \Xi^- p, \Lambda\Lambda) \cdot d\Omega_{CDS-eff} \cdot Br$$

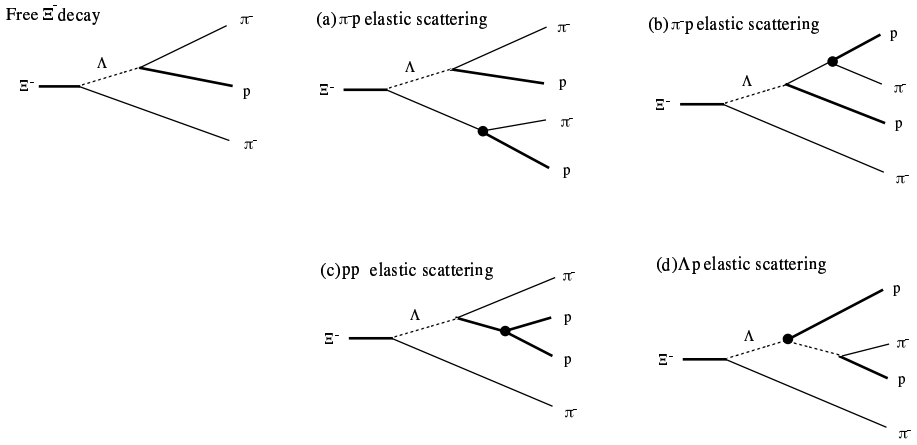

Figure 7: Possible sources of backgrounds: One of Ξ^- decay products scatters elastically with proton in the target, final particles of this event are two p's and two π^-'s same as Ξ^-p interactions.

n_{p-eff}	effective number of proton target in Ξ^- flight length
$\frac{d\sigma}{d\Omega}(\Xi^- p \to \Xi^- p, \Lambda\Lambda)$	differential cross sections uniform angular distribution, but as for the incident momentum dependence, the Kyoto-Niigata model RGM-F is assumed [18] For example at 700 MeV/c, 21.9 mb for Ξ^-p $\to \Xi^-$p , and 9.8 mb for Ξ^-p $\to \Lambda\Lambda$.
$d\Omega_{CDS-eff}$	effective solid angle of the CDS i.e. effective geometry for charged particles covered by the CDS, which is estimated by a simulation
Br	total branching ratio of decays to charged particles: $\cdot Br\,(\Xi^- \to \Lambda\pi^-) \times Br\,(\Lambda \to p\pi^-)$ for elastic scattering $\cdot\,[Br\,(\Lambda \to p\pi^-)]^2$ for$\Xi^- p \to \Lambda\Lambda$reactions

About 78000 Ξ^-p elastic scattering and 37000 Ξ^-p$\to \Lambda\Lambda$ reactions will occur in 100 days in the liquid hydrogen target. If we require that events should have 4 charged-particles' trajectories by the CDS as explained in the previous section, 10% of the Ξ^-p elastic scattering and 8.8% of Ξ^-p$\to \Lambda\Lambda$ reactions are remained. After the invariant mass analysis for the assignment of the final state and the elimination of backgrounds, we can expect 3650 elastic scatterings and 850 Ξ^-p$\to \Lambda\Lambda$ reactions. Fig. 9 shows a practical covered region by a simulation of this Ξ^-p experiment as a scatter plot for the Ξ^- incident momentum (just before scattering) vs. cosine of the scattering CM angle. If we assume 0.64 for the analysis efficiency (0.8 for the K^+ spectrometer side and 0.8 for the CDS side), the number of the Ξ^-p elastic scattering and the Ξ^-p$\to \Lambda\Lambda$ reaction will be finally about 2300 and 550, respectively.

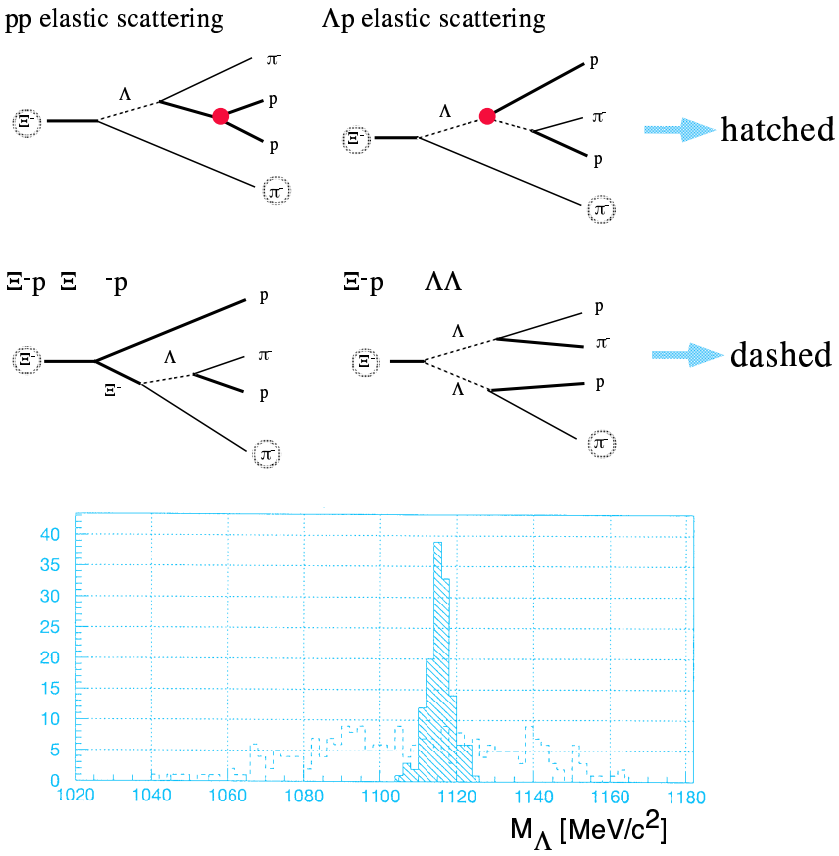

Figure 8: Mass spectrum of decay "Λ" from Ξ^- obtained by using the initial Ξ^- momentum from the (K^-,K^+) reaction and the momentum of one of π^- in the final particles detected by the CDS, under the assumption of Ξ^- free decay without scattering: (hatched) "Λ" mass obtained from Ξ^- free decay for (c) and (d) in Fig. 7, (dashed) "Λ" mass obtained from real Ξ^-p interactions.

As for the Ξ^-p→ ΛΛ reaction, the covered region of the ΛΛ invariant mass is from 2270 MeV/c^2 to 2410 MeV/c^2 as shown in Fig. 10. The positions of enhancement reported up to now is also displayed in the figure. In the differential cross sections, statistical errors will be about 10% with $\Delta(\cos(\theta))$= 0.2 binning.

4 Asymmetry in Λp and Σ^+p elastic scatterings

4.0.1 Physics interests

In the hyperon-nucleon interaction, a remarkable feature is the existence of the anti-symmetric spin orbit (ALS) interaction, proportional to $\sigma_n^1 - \sigma_n^2$, in addition to the symmetric (LS) term. This ALS term is not present in the nucleon-nucleon case due to charge symmetry. The cal-

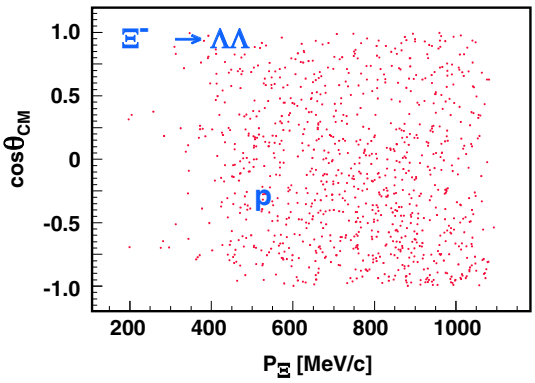

Figure 9: Practical covered region by a simulation of this Ξ^-pexperiment as a scatter plot for the Ξ^- incident momentum (just before scattering) vs. the scattering CM angle. The uniform angular distribution is used in the simulation.

culated spin-orbit strength shows difference between the OBE and the QCM [19]. Besides, large isospin dependence of the spin-orbit strength is expected for the Λ, Σ^+, and Σ^- -nucleon case [20]. In hypernuclei, both LS and ALS are important, since the spin-orbit strength in the folding model is proportional to the difference between the two (LS-ALS). A possible explanation of the observed small spin splitting of Λ-hypernuclei is a cancellation of LS and ALS strength, although each strength may not be so small [21].

An experimental study of the asymmetry measurement of Σ^+p elastic scattering (KEK-PS E452 [8]) has just finished its data acquisition. This experiment would give information on the spin-orbit interaction as a first step to some extent, however, statistics would not be sufficient and one should measure several polarization observables to provide unique and quantitative understanding of the spin orbit interaction. Direct measurements of some sets of polarization observables in the YN elastic scattering will give a stringent constraint to the present BB interaction pictures and give a pivotal information on the study of hypernuclei.

4.1 Experiment

In the spin-scattering matrix [22], the ALS term $\mathbf{b} \cdot (\sigma_n^1 - \sigma_n^2)$ remains in the hyperon-nucleon system as follows:

$$M = a + c\left(\sigma_n^1 + \sigma_n^2\right) + b\left(\sigma_n^1 - \sigma_n^2\right) m\sigma_n^1\sigma_n^2 + g\left(\sigma_P^1\sigma_P^2 + \sigma_K^1\sigma_K^2\right) + h\left(\sigma_P^1\sigma_P^2 - \sigma_K^1\sigma_K^2\right)$$

Measurements of both the polarization (P_y) and the analyzing power with the polarized target (A_y^T) give the efficient information of the ALS strength $\mathbf{b}$, since P_y and A_y^T are given by the following equations (2) and (3), respectively:

$$\begin{aligned} I_0 P_y &= \tfrac{1}{4} Tr\left(MM^\dagger \sigma_n^1\right), &&= 2Re\left[(a+m)\, c^* + (a-m)\, \mathbf{b}^*\right] &&= I_0 A_y \\ I_0 A_y^T &= \tfrac{1}{4} Tr\left(M\sigma_n^2 M^\dagger\right), &&= 2Re\left[(a+m)\, c^* - (a-m)\, \mathbf{b}^*\right] &&= I_0 P_y^T \end{aligned}$$

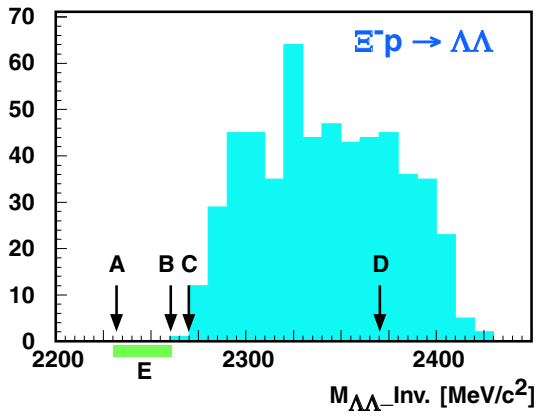

Figure 10: ΛΛ invariant mass for the Ξ^-p→ ΛΛ reaction. It covers from 2270 MeV/c^2 to 2410 MeV/c^2. A∼E in the figure represent the followings: A···2231.4 MeV/c^2 ($2m_\Lambda$), B···2259.6 MeV/c^2 ($m_{\Xi^-}+m_p$), Enhancements reported (as far as I know), C···2270 MeV/c^2 B.A.Shahbazian et al., Lett. al Nuovo Cimento 6 (1973) 63 D···2370 MeV/c^2 B.A.Shahbazian et al., Lett. al Nuovo Cimento 6 (1973) 63; P.Beilliere et al., Phys. Lett. 39B (1972) 671; not confirmed by G.Wilquet et al., Phys. Lett. 57B (1975) 97, E···2230 - 2260 MeV/c^2 J. K. Ahn et al., Phys. Lett. B444 (1999) 267.

Since weak decays of Σ^+ and Λ tell us their polarization, we don't need any polarimeter, fortunately. Therefore, in Λ, Σ^+ -proton scattering experiment, it is not so difficult to measure the polarization and the polarization transfer.

In the Λ and Σ^+ production reaction, produced hyperons are ideally polarized when one detect K^+ meson at finite angles around 30 degrees [23]. So, the same experimental setup for the measurement of Ξ^-p can be used to produce the polarized Λ and Σ^+. For Σ^-, there is no polarization information of its production, since the decay asymmetry of Σ^- hyperon is almost zero. So one cannot measure the polarization for Σ^-p elastic scattering. However, A_y^T can be measured like the Λ and Σ^+. If produced Σ^-'s at finite angle are polarized, measurement of the analyzing power will be also possible.

4.1.1 Expected yield

A detector design and simulation of the experiments for the polarization observables in the Yp elastic scattering is now in progress. Although a fast imaging device such as an image delay tube [24] and a new trigger system should be developed, yields can be estimated by using the preliminary numbers obtained in the E452 analysis. With the beam intensity of 10^7 π^+/spill at 1.7 GeV/c, about 10000 Λp and Σ^+p scattering is estimated within ten days beam time.

5 Summary

The coming 50 GeV machine will be a unique facility to perform the hyperon-proton (Yp) scattering experiment, while there were a lot of places for pp and pn cases. Two important experimental subjects are proposed here; Ξ^-p$\rightarrow \Lambda\Lambda$ reaction to study the $\Lambda\Lambda$ interaction directly, and asymmetry measurement in Λp and Σ^+ p elastic scatterings to investigate the anti-symmetric spin-orbit strength. The hyperons in several hundred MeV/c have short lifetimes of a few centimeters. There are two tractable ways to perform the Yp scattering experiment. One is to detect all the charged particles from the scattering and decay at some distance with a cylindrical chamber surrounding the target region, which is described in this letter of intent. Another is to observe hyperon-proton scattering directly in a small region with a vertex detector such as a scintillating fiber or a bubble chamber. This technique will be very important when we measure the Yp scattering at low energy region. However, at present, data acquisition rate of this type of detectors is strongly limited by a repetition rate of an imaging device. To utilize these vertex detector under intense beam at 50 GeV, technical R & D such as the image delay tube [24] should be started as soon as possible. These above methods are typical approaches for Yp scattering experiments.

Many and vigorous data of pp and pn scattering experiments in 50s and 60s was really important and indispensable to get the picture of NN interaction. BB studies will give more elementary understanding of nuclear force as baryon-baryon interaction and would reveal quark effect in hadronic phenomena.

References

[1] M. M. Nagels et al., Phys. Rev. D15 (1977) 2547; D20 (1979) 1633; P. M. Maessen et al., Phys. Rev. C40 (1989) 2226; Th. A. Rijken et al., Nucl. Phys. A547 (1992) 245c.

[2] B. Holzenkamp et al., Nucl. Phys. A500 (1989) 485; K. Holinde, Nucl. Phys. A547 (1992) 255c.

[3] M. Oka and K. Yazaki, Quarks and Nuclei, ed. W. Weise, Vol. 1 (World Scientific, 1984) 489; K. Yazaki, Nucl. Phys. A479 (1988) 217c; Perspectives of Meson Science, eds. T. Yamazaki, K. Nakai and K. Nagamine (Elsevier, The Netherlands, 1992) 795; K. Shimizu, Nucl. Phys. A547 (1992) 265c.

[4] U. Straub, Z. Y. Zhang, K. Bräuer, A. Faessler, S. B. Khadkikar, and G. Lübeck, Nucl. Phys. A483 (1988) 686; A508 (1990) 385c.

[5] Y. Fujiwara, C. Nakamoto, Y. Suzuki, Prog. Theor. Phys. 94 (1995) 214; 94 (1995)353; Phys. Rev. Lett. 76 (1996) 2242; Phys. Rev. C54 (1996) 2180.

[6] R. Engelmann et al. Phys. Lett. 21 (1966) 587; B. Sechi-Zorn et al. Phys. Rev. 175 (1968) 1735; G. Alexander et al. Phys. Rev. 173 (1968) 1452; J. A. Kadyk et al. Nucl. Phys. B27 (1971) 13; F. Eisele et al. Phys. Lett. 37B (1971) 204.

[7] J. K. Ahn et al., Nucl. Phys. A585 (1995)165c; A648 (1999) 263; Nucl. Instr. Meth. A457 (2001) 137; Y. Kondo et al., Nucl. Phys. A676 (2000) 371.

[8] E452 proposal at the KEK-PS; T. Kadowaki et al., to be published to European Physical Journal A.

[9] R. L. Jaffe, Phys. Rev. Lett. 38 (1977) 195.

[10] A. S. Carroll et al., Phys. Rev. Lett. 41(1978) 777; H. Ejiri et al., Phys. Lett. B228 (1989) 24; B. A. Shahbazian et al., Phys. Lett. 235 (1990) 208; K. Imai et al., Nucl. Phys. A547 (1992) 199c; A. Rusek et al., Phys. Rev. C52 (1995) 1580; S. Aoki et al., Phys. Rev. Lett. 65 (1990) 1729; J. K. Ahn et al., Phys. Lett. B378 (1996) 53.

[11] S. Aoki et al., Prog. Theor. Phys. 85 (1991) 1287.

[12] S. V. Bashinsky, R. L. Jaffe, Nucl. Phys. A625 (1997) 167; S. D. Paganis, T. Udagawa, G. W. Hoffmann, R. L. Ray, Phys. Rev. C56 (1997) 570.

[13] A. Ichikawa et al., Phys. Lett. B500 (2001) 37; H. Takahashi et al., Phys. Rev. Lett. 87 (2001) 212502-1.

[14] T. Fukuda et al., Nucl. Phys. A691 (2001) 220c.

[15] J. Nakano, Master Thesis (1996) unpublished.

[16] P928 proposal at the BNL-AGS.

[17] P. M. Dauber et al., Phys. Rev. 179 (1969) 1262.

[18] C. Nakamoto, private communication.

[19] A. Faessler, Nucl. Phys. A479 (1988) 3c; H. J. Pirner and B. Povh, Phys. Lett. 114B (1982) 308; A. Bouyssy, Nucl. Phys. A381 (1982) 445.

[20] K. Yazaki, Nucl. Phys. A479 (1988) 217c, K. Shimizu, Nucl. Phys. A547 (1992) 265c.

[21] C. Nakamoto, Y. Suzuki and Y. Fujiwara, Phys. Lett. B318 (1993) 587.

[22] N. Hoshozaki, Suppl. Prog. Theo. Phys. 42 (1968) 107.

[23] Candlin et al., Nucl. Phys. B226 (1983) 1; Haba et al., Nucl. Phys. B299 (1988) 627; R. D. Baker et al., Nucl Phys. B141 (1980) 29; D. X. Saxson et al., Nucl Phys. B162 (1980) 522.

[24] A. Berkovski et al., Nucl. Instr. and Meth. A380 (1996) 537.